IN-VENTO 2026
International Conference of the Italian Association for Wind Engineering
Bari, September 13th – 16th, 2026

A unified state-space model of aerodynamic forces on bridge decks

Matteo Pulvirenti[a], Luca Patruno[b], Simian Lei[c], Claudio Mannini[d], Vincent Denoël[e]

[a]*University of Liège, Liège, Belgium, Matteo.Pulvirenti@student.uliege.be*
[b]*University of Bologna, Bologna, Italy, luca.patruno@unibo.it*
[c]*University of Liège, Liège, Belgium, Simian.Lei@uliege.be*
[d]*University of Florence, Florence, Italy, claudio.mannini@unifi.it*
[e]*University of Liège, Liège, Belgium, v.denoel@uliege.be*

SUMMARY:
In bridge aerodynamics, motion-induced and buffeting forces are usually modeled in the frequency domain, which fails to capture non-stationary effects. This paper presents a State-Space Model (SSM) that generalizes available time-domain models, aiming to unify their formulation. In particular, motion induced forces are described by a system of differential equations, in which the differences from steady-state values are modeled as time-evolving variables. Additionally, the Frequency Response Function of the aforementioned system is evaluated, allowing for model calibration relying on flutter derivatives. Finally, an extension of the model to buffeting forces is introduced based on the concept of an effective velocity, providing an alternative perspective on available models that split between high and low frequency fluctuations. In this case, preliminary results obtained for the thin-airfoil show encouraging results.

Keywords: time-domain, state-space model, motion-induced forces, buffeting forces

1. INTRODUCTION

Modeling aerodynamic forces on bridge deck sections is of fundamental importance. These forces are typically categorized into static, motion-induced , and buffeting forces. Those two are commonly computed in the frequency domain; however, such a formulation fails to accommodate non-stationary events, such as non-synoptic winds. Available formulations to overcome this limitation are Rational Function Approximations (Barni et al., 2021) and Rheological Models (Diana et al., 2013).
Following these approaches, a set of differential equations that reproduces the Frequency Response Function (FRF), which links the deck motion to the aeroelastic forces, is built. Although these approaches have been successfully applied in various configurations, they have been mainly interpreted as ways to build surrogate models able to reproduce the FRF.
Aiming to shift the perspective toward a native time-domain approach and unify previous formulations, a State-Space Model for the calculation of motion-induced forces was proposed in (Lei et al., 2024). The model is based on quasi-steady theory, augmented by terms that represent the difference between the actual forces and their quasi-steady solutions. Such differences are modeled by appropriate differential equations. The model shows good performance for a selection of bridge decks.
Finally, aiming to extend the model to buffeting induced forces in a simple way, an effective velocity, representative of the relative motion between the deck and the surrounding fluid, is introduced, allowing for the reproduction of aerodynamic admittance with ease. In this case, preliminary analysis of a thin-airfoil shows encouraging results, providing an effective way to generalize the model for buffeting forces without relying on the usual splitting between high- and low-frequency fluctuations.

2. STATE-SPACE MODEL FOR MOTION-INDUCED FORCES

With reference to Fig. 1, the aerodynamic forces acting on the bridge deck are defined in terms of the relative velocity between the aerodynamic center and the incoming wind flow:

$$\mathbf{u}_r = \mathbf{u} - \frac{\mathrm{d}(B\mathbf{d})}{\mathrm{d}t}, \tag{1}$$

where $\mathbf{u}$ is the wind velocity vector in the x and y directions, B is the chord length, and $\mathbf{d}$ is the non-dimensional displacement vector of the aerodynamic center.

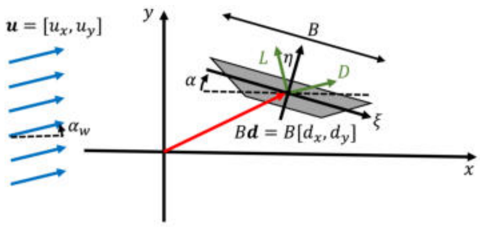

Figure 1. General formulation of the aerodynamic forces

The drag and lift forces are parallel and perpendicular to the direction of the relative wind flow, respectively, as shown in Fig. 1. To formulate these forces, the effective angle of attack α_e is defined as:

$$\alpha_e = \alpha + \alpha_{wr}, \quad \alpha_{wr} = \arctan\left(\frac{u_{r,y}}{u_{r,x}}\right), \tag{2}$$

where α is the deck rotation and α_{wr} is the inclination of the relative velocity vector on the x-axis. The quasi-static aerodynamic forces in the D-L (Drag-Lift) axes are:

$$\mathbf{F}_{a,st} = \begin{bmatrix} D \\ L \\ M \end{bmatrix} = \frac{1}{2}\rho U_r^2 \begin{bmatrix} BC_D(\alpha_e) \\ BC_L(\alpha_e) \\ B^2 C_M(\alpha_e) \end{bmatrix}, \quad \mathbf{C}_a^{eq} = \begin{bmatrix} C_D \\ C_L \\ C_M \end{bmatrix}, \tag{3}$$

where ρ is the fluid density, U_r is the magnitude of the relative velocity vector, and $\mathbf{C}_a^{eq}$ contains the static coefficients.

The state-space model (SSM) presented in (Lei et al., 2024) expresses the time-varying coefficients as:

$$\begin{cases} \dot{\mathbf{C}}_r(s) = \mathbf{A}\mathbf{C}_r(s) + \mathbf{B}\dot{\mathbf{e}}(s) \\ \mathbf{C}_a(s) = \mathbf{C}_a^{eq}(\alpha_e) + \mathbf{C}\mathbf{C}_r(s) + \mathbf{D}\dot{\mathbf{e}}(s), \end{cases} \tag{4}$$

where s is the non-dimensional time ($s = tU_r/B$), and the dot notation denotes the derivative with respect to s. The matrices $\mathbf{A}$, $\mathbf{B}$, $\mathbf{C}$, and $\mathbf{D}$ represent model coefficients, while $\mathbf{C}_r$ is the vector of aerodynamic states, which accounts for retarded contributions as corrections to the equilibrium $\mathbf{C}_a^{eq}$. The vector $\mathbf{e} = [\alpha, \dot{\alpha}, \dot{d}_y, \dot{d}_x]^T$ collects the kinematic parameters.
The model complexity is governed by the number of states n_{cr}. Denoting n_e and n_c as the lengths of vectors $\mathbf{e}$ and $\mathbf{C}_a$, those values can be adjusted to include or exclude d_x and C_D contributions.

In (Lei et al., 2024), a procedure to express aerodynamic forces as a function of a transfer function $\mathbf{H}(K)$ is described. The latter is derived from the SSM to compute the oscillating forces $\tilde{\mathbf{F}}$ under harmonic motions at reduced frequency $K = \omega B / U_r$:

$$\mathbf{F} = \bar{\mathbf{F}} + \tilde{\mathbf{F}} = \bar{\mathbf{F}} + \mathbf{H}(K) \begin{bmatrix} \tilde{d}_x \\ \tilde{d}_y \\ \tilde{\alpha} \end{bmatrix} e^{iKs}, \quad \mathbf{H}(K) = \begin{bmatrix} P_6^* + iP_5^* & P_4^* + iP_1^* & P_3^* + iP_2^* \\ H_6^* + iH_5^* & H_4^* + iH_1^* & H_3^* + iH_2^* \\ A_6^* + iA_5^* & A_4^* + iA_1^* & A_3^* + iA_2^* \end{bmatrix} K^2, \tag{5}$$

where $\bar{\mathbf{F}}$ represents the non-oscillating part for $\mathbf{F}$. The matrix $\mathbf{H}(K)$ contains the flutter derivatives (P_i^*, H_i^*, A_i^*) as detailed in (Lei et al., 2024).

3. MODEL CALIBRATION AND RESULTS

Since the matrix $\mathbf{H}(K)$ in Eq. (5) relates the flutter derivatives to the model parameters $\mathbf{A}$, $\mathbf{B}$, $\mathbf{C}$, and $\mathbf{D}$, a calibration procedure can be established to fit the model to experimental flutter derivatives. The model is calibrated by minimizing the error between measured and computed flutter derivatives from Eq. (5) using a BFGS algorithm.
An example of results obtained using the model is reported in Fig. 2, which presents the flutter derivatives as a function of the reduced velocity $U_{red} = 2\pi/K$. In this case, $n_e = 3$ and $n_c = 2$ are adopted (excluding d_x and C_D), resulting in a matrix $\mathbf{H}(K)$ of size 2×2. This formulation expresses the flutter derivatives H_i^* and A_i^* for $i = 1, \ldots, 4$.

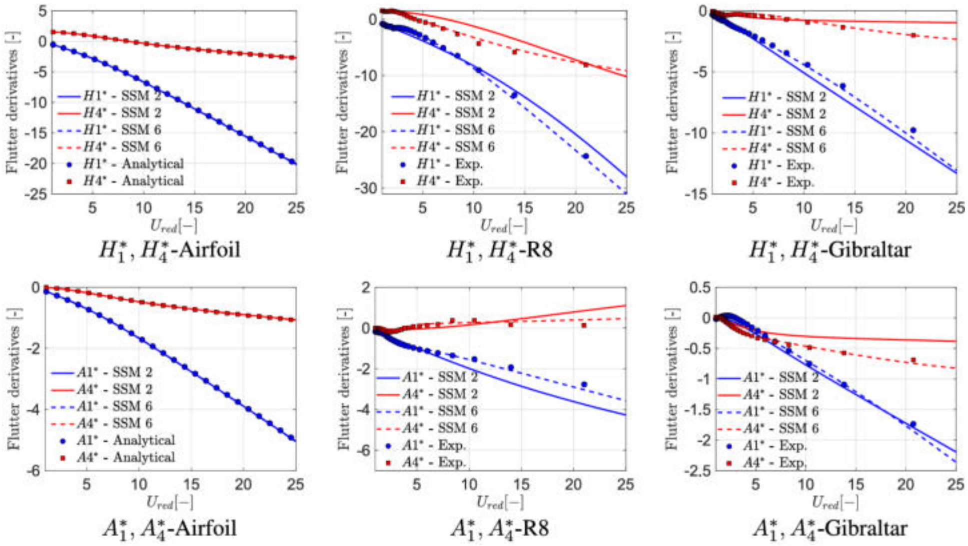

Figure 2. Comparison between experimental and model-reproduced flutter derivatives (2 and 6 state variables) for the thin-airfoil, the AR8 rectangular prism, and the Gibraltar Bridge section. (Lei et al., 2024)

4. EXTENSION TO BUFFETING FORCES

The model developed for buffeting forces is an extension of the previous one. The idea is to introduce an effective vertical velocity (v_{eff}) in the vector $\mathbf{e}$ such that $\mathbf{e} = \begin{bmatrix} \alpha & \dot{\alpha} & (\dot{d}_y - v_{eff}) \end{bmatrix}^T$. This velocity physically translates to the vertical velocity that the body is actually experiencing. This intuition comes from the fact that lift takes time to develop when the body is subject to a gust, as shown in (Scanlan, 1993). The quantity v_{eff} is computed with an additional SSM:

$$\begin{cases} \dot{\mathbf{v}}_r(s) = \mathbf{A}_v \mathbf{v}_r(s) + \mathbf{B}_v \dot{v}(s) \\ v_{eff}(s) = v(s) - \mathbf{C}_v \mathbf{v}_r(s), \end{cases} \tag{6}$$

where $v = u_y/U$ is the non-dimensional vertical velocity (with U being the mean velocity in the x direction), $\mathbf{v}_r$ is the state vector, and $\mathbf{A}_v$, $\mathbf{B}_v$, and $\mathbf{C}_v$ represent matrices collecting model coefficients. The length of $\mathbf{v}_r$ is n_v, such that $\mathbf{A}_v$ is of size $n_v \times n_v$, $\mathbf{B}_v$ is $n_v \times 1$, and $\mathbf{C}_v$ is $1 \times n_v$. Again, n_v defines the level of complexity of this model.

A first result for the thin-airfoil is shown in Fig. 3. The model is first calibrated against the Theodorsen function to obtain the matrices $\mathbf{A}$, $\mathbf{B}$, $\mathbf{C}$, and $\mathbf{D}$, as shown in Fig 2. Then, we calibrate $\mathbf{A}_v$, $\mathbf{B}_v$, and $\mathbf{C}_v$ so that, the overall model reproduces the Sears function.

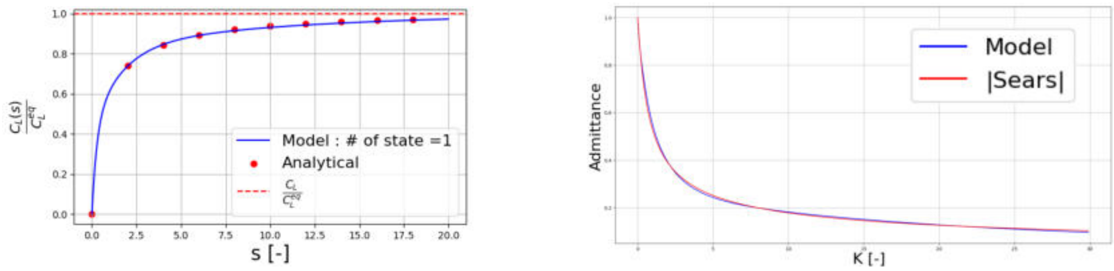

(a) Comparison between theoretical (Küssner function) and model-reproduced indicial function for the thin-airfoil.

(b) Comparison between theoretical (Sears function) and model-reproduced admittance for the thin-airfoil.

Figure 3. Calibrated model for buffeting forces for the thin-airfoil

Similar to Eq. (5), it is possible to link the model coefficient matrices of Eq. (6) to its transfer function $H_t(K)$. The latter allows the computation of the amplitude of the oscillating force in the y direction, $\tilde{F}_y$, in response to a harmonic gust with the amplitude $\tilde{v}$ at frequency K:

$$\tilde{F}_y = \frac{1}{2}\rho B U^2 H_t(K)\,\tilde{v}, \qquad \chi_v(K) = \frac{H_t(K)}{C_L' + C_D}, \tag{7}$$

where $\chi_v(K)$ is the lift admittance function, and C_L' is the derivative of the lift coefficient with respect to the angle of attack. The matrices $\mathbf{A}_v$, $\mathbf{B}_v$, and $\mathbf{C}_v$ can be calibrated using experimental data of $\chi_v(K)$ for any aerodynamic sections.

5. CONCLUSIONS

This study presents a time-domain state-space framework for modeling aerodynamic forces on bridge decks. The motion-induced force model was successfully validated, reproducing flutter derivatives for various geometries with few state variables. The extension of the approach to buffeting forces produces consistent results between the Sears function and the admittance obtained from the Theodorsen function combined with the response function of the effective velocity if a single additional state is considered for the latter. Future developments will be devoted to testing the model performance on practical cases showing more complex aerodynamic behavior.

REFERENCES

Barni, N., O. Øiseth, and C. Mannini (2021). Time-Variant Self-Excited Force Model Based on 2D Rational Function Approximation. Journal of Wind Engineering and Industrial Aerodynamics 211, 104523.

Diana, G., D. Rocchi, and T. Argentini (2013). An experimental validation of a band superposition model of the aerodynamic forces acting on multi-box deck sections. Journal of Wind Engineering and Industrial Aerodynamics 113, 40–58.

Lei, S., L. Patruno, C. Mannini, S. D. Miranda, and Y. Ge (2024). Time-domain state-space model formulation of motion-induced aerodynamic forces on bridge decks. Journal of Wind Engineering and Industrial Aerodynamics 255, 105937.

Scanlan, R. H. (1993). Problematics in formulation of wind-force models for bridge decks. Journal of Engineering Mechanics 119, 1353–1375.